Title	Porphyrin Molecules Working as Nanodevice on Single-Walled Carbon Nanotube Wiring
Author(s)	Tanaka, Hirofumi; Yajima, Takashi; Matsumoto, Takuya et al.
Citation	Advanced Materials. 2006, 18(11), p. 1411-1415
Version Type	AM
URL	https://hdl.handle.net/11094/3267
rights	
Note	

Porphyrin Molecules Working as Nanodevice on Single-Walled Carbon Nanotube Wiring **

Hirofumi Tanaka, Takashi Yajima, Takuya Matsumoto, Yoichi Otsuka, and Takuji Ogawa[*]

keywords: carbon nanotube wiring, PCI-AFM, rectification, molecular device, self-assembly

---

[*] Dr. H. Tanaka§, T. Yajima, Prof. T. Ogawa§

Research Center for Molecular-Scale Nanoscience, Institute for Molecular Science.

5-1 Higashiyama, Myodaiji, Okazaki 444-8787, Japan.

E-mail: htanaka@ims.ac.jp, ogawat@ims.ac.jp.

Y. Otsuka and Prof. Matsumoto§

The Institute of Scientific and Industrial Research, Osaka University.

8-1 Miohogaoka, Ibaraki, 567-0047, Japan.

§ CREST, Japan Science and Technology Corporation.

[* *] This work was supported by Grants-in-Aid for Scientific Research (Nos.15201028 and 14654135) from the Ministry of Education, Culture, Sports, Science, and Technology of Japan. One of the authors (HT) thanks Visionarts Inc. for financial support.

For the future development of molecular electronics, we should construct nanosized molecular devices placed on nanowiring. To obtain high-quality devices composed of a few molecules, the wiring and the device should be connected well to maintain a constant interface. For this purpose, a single-walled carbon nanotube (SWNT)/porphyrin complex was prepared and then its electronic property was investigated while observing a topographic image using point-contact current imaging atomic force microscopy (PCI-AFM). Using PCI-AFM, we can measure the current along the long axis of the wiring by which the quality of the device in the circuit can be determined. The I-V curves were asymmetric with respect to the origin where an aggregate of several porphyrin molecules was absorbed, while they were symmetric without them. This means the porphyrin aggregation works as a rectification device on SWNT wiring. This is the first study which proves the electronic property of a few porphyrin molecules absorbed on SWNT.

Although many researchers have reported the conductivity of nanostructures using nanometer-size gaps (nanogaps) fabricated by e-beam lithography,[1] break junctions,[2] free-standing carbon nanowires,[3] electrochemical growth,[4] carbon nanotube masking[5] and electromigration,[6] it is very hard to observe whether the object contacts the electrode stably when the size of the object is less than 10 nm.[7] For example, if a particle of less than 10 nm diameter is placed between electrodes with a gap of a few nm on a substrate, we have no chance to observe whether the particle connects stably to the electrodes, because the tip of the scanning probe microscope (SPM) cannot reach inside the gap, and the resolution of scanning electron microscopy (SEM) is not sufficient to observe it. From the results of the measurement of the nanogap electrode, it is doubtful whether the conduction of the molecule was really measured, since a molecule was not observed during the measurement.

A key technique to solve the above problem is the PCI-AFM developed by Matsumoto *et al.* [8-10] This technique causes less damage to the surfaces of the tip and sample during scanning than contact-mode AFM in principle. The advantage of PCI-AFM is that soft materials, such as polymers (wires), can avoid being swept out by the scanning tip. We can also detect differences in electric property on the nanoscale by PCI-AFM because topographic images and current-voltage (I-V) curves can be obtained simultaneously.

Another key method of solving the above problem is to use an SWNT as an electrode ("SWNT-electrode method"). An SWNT is an excellent electrode for measurement on the nanoscale because it is the only high-conductivity material whose diameter is approximately 1 nm and because it is easy to observe the sample on the SWNT by AFM. By combining these two techniques, we can measure current along the long axis of an object while observing the topological images of the target. Since variable molecules can be absorbed on the SWNT,[11-12] the combined technique can be used to measure the electric properties of different types of molecular devices.

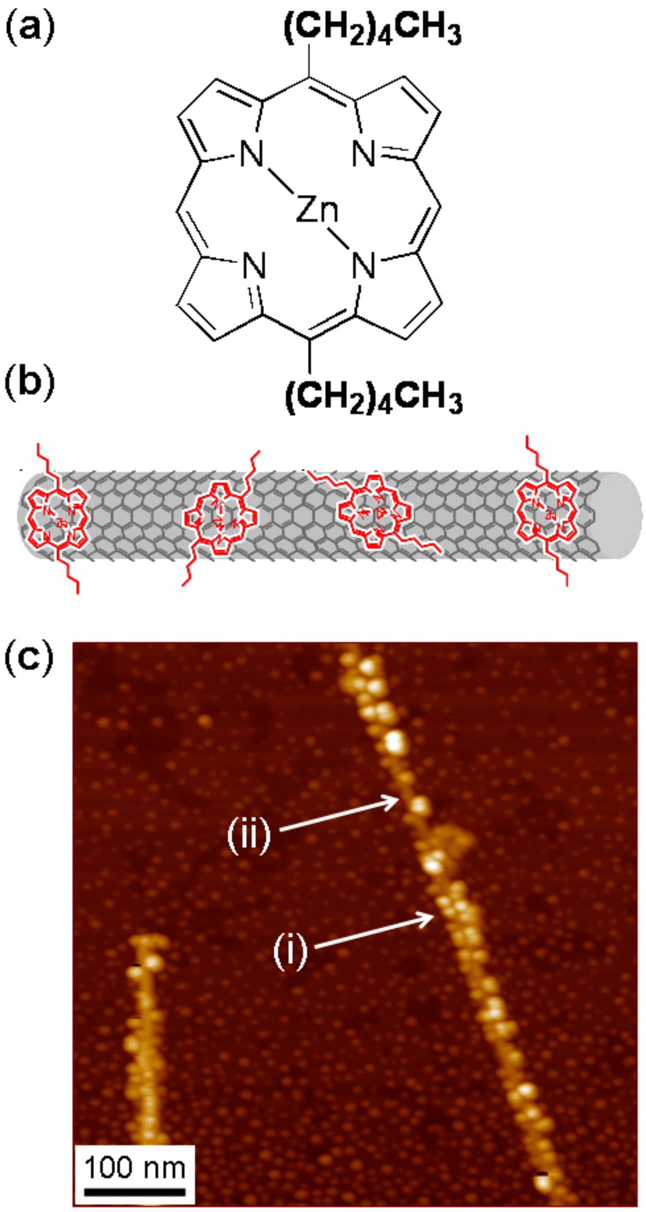

Fig. 1 H. Tanaka *et al.*

We synthesized 5,15-Bispentylporphyrinato zinc(II) (**BPP-Zn**) (Fig. 1(a)) having two pentyl groups to increase the solubility of the complex with an SWNT (Fig. 1(b)) in organic solvent. SWNTs were added to a dimethyl formamid (DMF) solution of **BPP-Zn** (0.1 mM, 5 mL), and then sonicated for 30 min. The solution was centrifuged at 1000 G and the supernatant was collected. The SWNT/**BPP-Zn** complex was collected using a filter (0.5 μm, MILIPORE) and excess **BPP-Zn** was removed by rinsing with $CHCl_3$ (100 mL). SWNT/**BPP-Zn** was added to DMF (2 mL) and the solution was sonicated for 30 min. The SWNT/**BPP-Zn** complex was very stable as no precipitation was observed in the solution even after being left for one month at room temperature. The obtained solution was cast on a mica substrate and the surface was observed by tapping-mode AFM.

Figure 1(c) shows an AFM image of the complex on the substrate. The aggregation of the SWNT/**BPP-Zn** complex having a thickness of 2.5-4.5 nm was observed on the SWNT as white dots. Excess **BPP-Zn** molecular aggregations were also observed on the whole substrate. This is the first time that porphyrin molecules were observed absorbing on an SWNT by AFM. From the image, it can be seen that the **BPP-Zn** strongly binds to the SWNT. Since the diameter of the SWNT is approximately 1.1-1.5 nm, the thickness of the **BPP-Zn** aggregate is calculated to be approximately 1-3 nm. White dots observed both on the SWNT and on the substrate are estimated to be composed of aggregates of several **BPP-Zn** molecules. Almost all of the parts of the SWNT were covered by **BPP-Zn**, indicated by arrow (i). However, some exposed parts of the SWNT are also observed, indicated by arrow (ii).

A gold electrode was deposited on half of the substrate with the other half of the substrate covered with a cover glass to avoid Au deposition. Au was deposited onto the substrate by thermal vacuum deposition. The thickness of the deposited Au layer was approximately 40 nm. By removing the cover glass carefully, an electrode with a sharp edge was obtained with no diffusion (see inset in Fig. 2). For the *I-V* measurement, we used PCI-AFM whose procedure is shown in Fig. 2. The PCI-AFM measurement was conducted using JEOL JSPM-4210 expanded with two function generators (WF1946, NF Corporation). Pt-coated conductive cantilevers were used to measure current. The force constant and resonant frequency of the cantilevers were 4.5 N/m and approximately 150 kHz, respectively. This measurement was performed in a nitrogen-gas-purged atmosphere to avoid humidity. When *I-V* measurement was carried out, the force between the cantilever and the sample was approximately 13 nN, calculated using a force curve.[9] Bias voltage was applied to the gold electrode on the substrate and the cantilever was grounded.

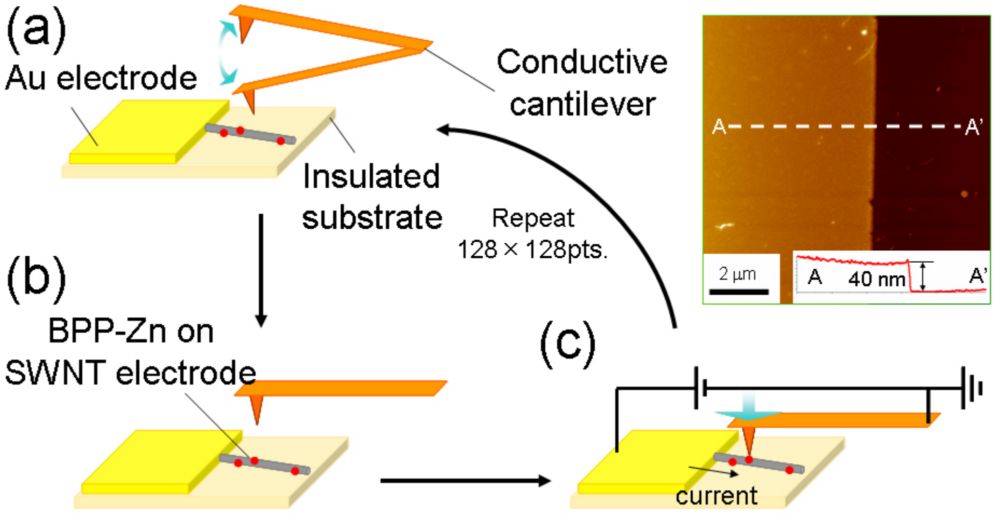

Fig. 2 H. Tanaka *et al.*

Figure 3(a) shows a topographic image of the complex obtained by PCI-AFM. Points A'-G' indicate the position where the *I-V* curve is compared. **BPP-Zn** aggregates having approximately 3 nm thickness were absorbed on the surface of a bundle of SWNTs (b-SWNTs) having approximately 2.5 nm thickness. Since the average diameter of a single SWNT (s-SWNT) is 1.1 nm (from the product sheet; Sigma Aldrich), the b-SWNT consists of two s-SWNTs. Since the height of the **BPP-Zn** is approximately 0.35 nm, the **BPP-Zn** aggregate is assumed to be constructed of several **BPP-Zn** molecules aggregating at one position. For every point of 128 ×128 dots in Fig. 3(a), an *I-V* curve and an AFM topographic image were simultaneously obtained. At points B', C' and F' (N-points as no-porphyrin-points, hereafter), non-ohmic *I-V* curves symmetric with respect to the origin were obtained from an exposed b-SWNT. At points A', D', E' and G' (P-points as porphyrin-points, hereafter), *I-V* curves asymmetric with respect to the origin were obtained from a **BPP-Zn** aggregate on the b-SWNT. Apparently, the current at the positive voltage at the P-points is much lower than that taken at the N-points or that in the range of negative voltage. The current through the **BPP-Zn** aggregate has been distinguished from that through the contact point of Pt and the SWNT on the nanoscale. By normalizing the *I-V* curves at -1.5 V, all the curves from points A'-F' were perfectly coincident in the range of $V < 0$. On the other hand, in the range of $V > 0$, they are grouped into two types: symmetric curves obtained at the N-points and asymmetric curves with respect to the origin obtained at P-points showing rectification.

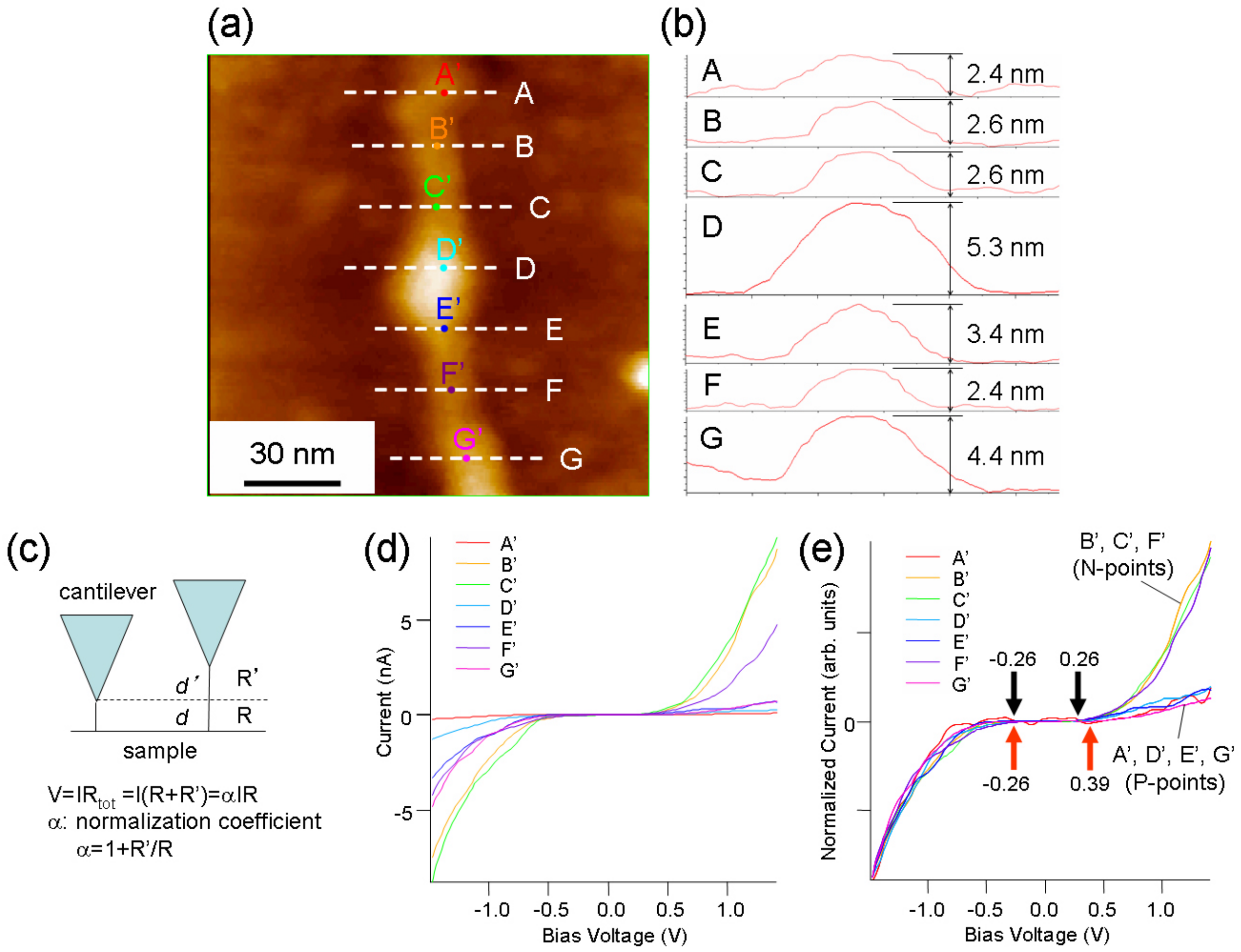

Fig. 3 H. Tanaka *et al.*

To discuss the normalization, it is necessary to know the distance between Pt and the sample (Fig. 3(c)) because the *I*-*V* curves obtained are unbraided (Fig. 3(d)). The total contact resistance between a sample and a cantilever is expressed as the sum of the contact resistance for a certain distance between the SWNT and Pt (*R*), and additional tunnel resistance incurred by the gap from the position (*R'*) because of an increased tunnel gap. Current passing through the interface is thus expressed as

$$V = I(R+R') = \alpha IR, \ \alpha = 1+R'/R \qquad (1)$$

R should be constant and α is a normalizing coefficient (Fig. 3(c)). If we know *α* here, we can obtain the ratio of *R'* of each point. *R*' is due to the contact between the electrode and the sample. The *α* values are 38.4, 1.1, 1.0, 6.9, 2.6, 2.1 and 2.8 for points A'-F', respectively. The tunnel distance approximately changes as $d' \approx \mathrm{Log}(\alpha)$. By comparing *d'*, the difference in *d'* between points A and C is approximately

0.16 nm, and that between points D’ and C’ is 0.08 nm. Although this estimation is based on the assumption that **BPP-Zn** works just as a tunnel gap, the contact condition of each point can be estimated relatively. Concluding from the results described above, such a small height variation does not affect the conduction mechanism.

Figure 3(e) shows that this SWNT exhibits semiconductor conduction with a narrow band gap. Two black arrows indicate the band edge of the object. The band edge of the conduction band (CB) is at approximately 0.26 V and that of the valence band (VB) is at -0.26 V. The band gap of approximately 0.52 *e*V corresponds to the energy gap obtained in a previous study.[13] Note that the curve obtained from the exposed SWNT is influenced by the absorbed porphyrin and is different from that obtained in reported studies[14] for an ideal SWNT. On the other hand, the orbital of the **BPP-Zn** hybridized with that of the SWNT in CB is at approximately 0.39 V and that in VB is at approximately -0.26 V. The band gap of the SWNT on which porphyrin is absorbed is expected to be approximately 0.65 *e*V. This band gap is wider than that of the exposed SWNT because of the orbital hybridization of the SWNT and porphyrin.

By analyzing the shape of the *I-V* curve, it can be seen that the conducting property is Fowler-Nordheim (FN) tunneling[15] because the *I-V* curve is fit using the following equation; [16]

$$I(V) = A^{*}V^{2}\exp(-B/V) \qquad (2)$$

where A and B are constants and V is the applied voltage to the SWNT. By comparing B values of the equation, we can compare the conduction property at N-points and P-points, because B is related to the barrier heights of Pt and the SWNT.[16] By fitting the measured *I-V* curves at positive bias to FN theory, the B were 1.17 ± 0.31 V for N-points and 1.71 ± 1.40 V for P-points. We can conclude that B at P points is approximately 1.5 times larger than that at N-points.

We can discuss the electric properties of porphyrin on the SWNT electrode from the results described above; the red arrow at 0.39 V shown in Fig. 3(e) is expected as a band edge (BE) from the hybridized orbital of the CB of SWNT and that of **BPP-Zn**. This BE is slightly higher than that of the SWNT shown in Fig. 3(e) at 0.26 V. The BE of SWNT/**BPP-Zn** in VB are expected to be laid at the same level as that of the SWNT (-0.26 V) because all *I-V* curves agree below 0 V.

Figure 4 shows a summarized scheme of the band structure at the interface of SWNT/ Pt and SWNT/ **BPP-Zn**/ Pt. When **BPP-Zn** attaches to a cantilever (Pt), a strong interaction occurs to transfer a charge from **BPP-Zn** to SWNT. Here, **BPP-Zn** is positively charged, which is the reason the work function is aligned at the interface between **BPP-Zn** and Pt because of electric polarization. Then, the energy level of Pt is aligned with the lower level at the interface between **BPP-Zn** and Pt. This type of phenomenon is reported as a results of UV photoemission spectroscopy (UPS).[17-18]

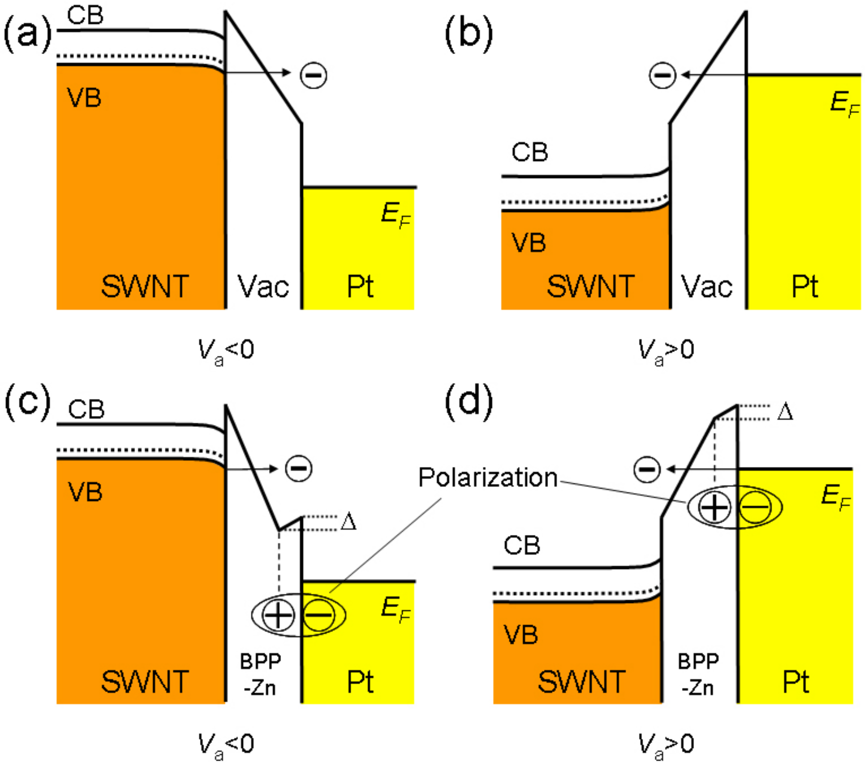

Fig. 4 H. Tanaka *et al.*

The mechanism of electron conduction in this system is thought to be tunneling as described above. A change in conduction by absorbing **BPP-Zn** is induced by a change of band around a tunneling area because of the strong correlation between Pt and **BPP-Zn**. By the shape of the *I-V* curve at the P-points, the conducting property is found to be similar to the tunneling of the N-points in the negative bias, since the normalized *I-V* curve is coincident with that of the exposed SWNT. Accordingly, the potential barrier in Fig. 4(c) is similar to that in Fig. 4(a) although the potential barrier slightly becomes narrower.

On the other hand, the conduction was restrained in the positive bias. An electron is affected by the wider potential barrier like that shown in Fig. 4(d), which stops the electron from passing through the potential.

In conclusion, a porphyrin aggregate of even 2-3 nm size behaved as a rectification device on the SWNT. It is very effective to combine the SWNT-electrode method and PCI-AFM for the current measurement of single or several molecules. This combination allows simultaneous observation of the topography of molecules on the electrode during measurement. Using this technique, electric conduction property at the interface of SWNT/ Pt and SWNT/ **BPP-Zn**/ Pt was distinguished in the nanoscale, that is; a nanorectification device is spontaneously controlled for placement on the SWNT by synthesis.

References

[1] A. Bezryadin; C. Dekker; G. Schmid, *Appl. Phys. Lett.* **1997,** 71, 1273.

[2] C. J. Muller; J. M. Vanruitenbeek; L. J. Dejongh, *Phys. Rev. Lett.* **1992,** 69, 140.

[3] A. Bezryadin; C. Dekker, *J. Vac. Sci. Technol. B* **1997,** 15, 793.

[4] A. F. Morpurgo; C. M. Marcus; D. B. Robinson, *Appl. Phys. Lett.* **1999,** 74, 2084.

[5] J. Lefebvre; M. Radosavljevic; A. T. Johnson, *Appl. Phys. Lett.* **2000,** 76, 3828.

[6] H. Park; A. K. L. Lim; A. P. Alivisatos; J. Park; P. L. McEuen, *Appl. Phys. Lett.* **1999,** 75, 301.

[7] H. W. Zandbergen; R. J. H. A. van Duuren; P. F. A. Alkemade; G. Lientschnig; O. Vasquez; C. Dekker; F. D. Tichelaar, *Nano Lett.* **2005,** 5, 549.

[8] Y. Otsuka; Y. Naitoh; T. Matsumoto; T. Kawai, *Jpn. J. Appl. Phys. 2* **2002,** 41, L742.

[9] Y. Otsuka; Y. Naitoh; T. Matsumoto; T. Kawai, *Appl. Phys. Lett.* **2003,** 82, 1944.

[10] A. Terawaki; Y. Otsuka; H. Y. Lee; T. Matsumoto; H. Tanaka; T. Kawai, *Appl. Phys. Lett.* **2005,** 86.

[11] J. Chen; H. Liu; W. A. Weimer; M. D. Halls; D. H. Waldeck; G. C. Walker, *J. Am. Chem. Soc.* **2002,** 124, 9034.

[12] H. Murakami; T. Nomura; N. Nakashima, *Chem. Phys. Lett.* **2003,** 378, 481.

[13] J. W. G. Wildoer; L. C. Venema; A. G. Rinzler; R. E. Smalley; C. Dekker, *Nature* **1998,** 391, 59.

[14] R. Saito; M. Fujita; G. Dresselhaus; M. S. Dresselhaus, *Appl. Phys. Lett.* **1992,** 60, 2204.

[15] R. H. Good, Jr; E. W. Muller *Handbuch der Physik*; Springer-Verlag: Berlin, 1956; Vol. XXI, 176.

[16] D. G. Xu; G. D. Watt; J. N. Harb; R. C. Davis, *Nano Lett.* **2005,** 5, 571.

[17] S. Narioka; H. Ishii; D. Yoshimura; M. Sei; Y. Ouchi; K. Seki; S. Hasegawa; T. Miyazaki; Y. Harima; K. Yamashita, *Appl. Phys. Lett.* **1995,** 67, 1899.

[18] K. Seki; E. Ito; H. Ishii, *Synth. Met.* **1997,** 91, 137.

FIGURE CAPTIONS.

Figure 1. (a) Structural formula of synthesized 5,15-Bispentylporphyrinato zinc(II) (**BPP-Zn**) (b) Model of SWNT/ BPP-Zn complex (c) Tapping-mode AFM image of **BPP-Zn** on SWNT electrode. Surplus **BPP-Zn** can also be observed on the whole substrate. Almost all of the SWNT was covered by **BPP-Zn** aggregates, indicated by arrow (i). Some parts of the SWNT were partially exposed, indicated by arrow (ii).

Figure 2. Procedure of PCI-AFM method. (a) A topographic image was obtained by tapping-mode AFM. (b) The vibration of the cantilever was stopped to measure the *I-V* curve. (c) The AFM tip was pressed to the sample to make electrical contact, and then the *I-V* curve was measured. Steps (a)-(c) were repeated every 128 × 128 points of the AFM image. The inset shows an AFM image of the Au electrode and its height profile. A sharp edge 40 nm high was formed.

Figure 3. (a) Topographic image of **BPP-Zn** absorbed on SWNT electrode. The *I-V* measurement was performed at points A'-G'. (b) Cross section of each line in Fig. 3(a). (c) Relation between a tunnel resistance and a distance of sample and cantilever. (d) *I-V* curves obtained at each point. (e) The *I-V* curves were normalized at -1.5 V. All curves are coincident below 0 V. I-V curves are classified into two types over 0 V. One is symmetrical with respect to the origin where no porphyrin is absorbed and another is asymmetrical where porphyrin is absorbed. Two types of arrow indicate the band edges (BE) of the objects. Black and red arrows indicate the BE of the object for N-points and P-points, respectively.

Figure 4. Schematic band structures of SWNT and Pt summarized by *I-V* analysis in the range of (a) negative sample bias and (b) positive bias. A tunnel gap exists between Pt and the SWNT (Vac). Electrons tunnel the triangular potential barrier at the valence band of the SWNT. After **BPP-Zn** is absorbed on the SWNT, schematic band structures changed to (c) in negative sample bias and (d) in positive bias. The band of the tunneling area changed because the energy level aligned lower (Δ) at the interface between **BPP-Zn** and Pt[17-18] because of polarization at their interface. Electrons feel a

narrower potential barrier than the triangular potential in (c) and a wider potential barrier in (d), respectively, which is the reason for the asymmetric *I*-*V* curves.